Table 1 Frequency parameter λ

S.No.	k	α	λ mean (Ref.4)	One-term approx. [Eq. (5)]	% Error	Two-term approx. [Eq. (7)]	% Error
		0.1	167.657	168.053	0.236	167.660	0.0017
		0.2	183.581	185.173	0.867	183.600	0.0103
		0.3	199.972	203.560	1.794	200.037	0.0327
		0.4	217.082	223.213	2.824	216.990	−0.0424
1	0.5	0.5	234.215	244.133	4.235	234.480	0.1132
		0.6	251.944	266.320	5.706	252.528	0.2317
		0.7	270.139	289.773	7.268	271.152	0.3752
		0.8	288.786	314.492	8.901	290.373	0.5495
		0.1	429.344	430.366	0.238	429.355	0.0026
		0.2	470.539	474.641	0.872	470.601	0.0133
		0.3	513.154	522.456	1.813	513.413	0.0505
		0.4	557.195	573.813	2.982	557.850	0.1175
2	1.0	0.5	603.011	628.711	4.262	603.969	0.1589
		0.6	650.051	687.150	5.707	651.829	0.2735
		0.7	698.483	749.129	7.251	701.485	0.4298
		0.8	748.214	814.651	8.879	752.988	0.6381

Table 2 Loss factor ratio η_V/η_C

S. No.	k	α	η_V/η_C [Eq. (11)]	η_V/η_C (one-term approx.)	η_V/η_C (two-term approx.)
		0.1	0.9782	0.9786	0.9842
		0.2	0.9573	0.9579	0.9701
		0.3	0.9374	0.9387	0.9566
		0.4	0.9184	0.9202	0.9441
1	0.5	0.5	0.9002	0.9026	0.9326
		0.6	0.8830	0.8859	0.9212
		0.7	0.8666	0.8702	0.9107
		0.8	0.8509	0.8553	0.9005
		0.1	0.9781	0.9783	0.9840
		0.2	0.9571	0.9576	0.9696
		0.3	0.9368	0.9383	0.9563
		0.4	0.9175	0.9198	0.9439
2	1.0	0.5	0.8991	0.9022	0.9322
		0.6	0.8815	0.8855	0.9208
		0.7	0.8647	0.8698	0.9101
		0.8	0.8487	0.8545	0.8997

V. Conclusions

For the purpose of analysis, a steel plate of SAE 1020 was considered, having a thickness of $h_0 = 0.1$ in. (0.0025m) and damping properties[2] J and N as 2.626×10^{-13} and 2.286, respectively, and subjected to a central point load of 0.2248 lb (1N). Fundamental mode loss factors were computed for the various combinations of the aspect ratios and taper parameters.

Table 1 shows the values of the frequency parameters for two representative cases. It is observed that the two-term solution gives a fairly accurate value of the natural frequency, and the loss factors calculated at these values of the resonant frequencies would not be far-off from the actual values. Table 2 shows the values of the loss factors as calculated by one-term and two-term approximations, and as obtained from Eq. (11). It is seen that Eq. (11) gives a value of loss factor which is within a maximum of 5% of the two-term approximation. Hence, this could be used for obtaining an estimate of the fundamental mode internal loss factor of the plate.

References

[1] Ver, I. L. and Holmer, C. I., "Interaction of Sound Waves with Solid Structures," *Vibration and Noise Control*, edited by L. L. Beranek, 1st ed., McGraw-Hill, New York, 1971, pp. 331-333.

[2] Lazan, B. J., *Damping of Materials and Members in Structural Mechanics*, 1st ed., Oxford-Pergamon, New York, 1968.

[3] Leissa, A. W., *Vibration of Plates*, SP-160, 1969, NASA.

[4] Appl, F. C. and Byers, N. R., "Fundamental Frequency of Simply Supported Rectangular Plates of Linear Varying Thickness," *Journal of Applied Mechanics*, Vol. 32, 1965, pp. 163-167.

[5] Kantorovich, L. V. and Krylov, V. I., *Approximate Methods of Higher Analysis*, 3rd ed., Interscience, New York, 1964, pp. 258-262.

Hypersonic Flow over Concave Surfaces with Leading-Edge Bluntness

A. V. Murthy*
National Aeronautical Laboratory, Bangalore, India

Introduction

THE study of leading-edge bluntness effects at hypersonic speeds on surfaces other than a flat plate or a convex afterbody shape has not received much attention in the literature. The nature of the downstream effect of the leading-

Received September 25, 1974; revision February 21, 1975. The author wishes to express his thanks to J. F. Clarke and J. L. Stollery, both of Cranfield Institute of Technology, Bedford, England for helpful discussions.

Index category: Supersonic and Hypersonic Flow.

*Scientist, Aerodynamics Division.

edge bluntness depends much on the afterbody shape. In particular, when the afterbody is a concave surface the flow is quite complicated because of the interaction between the leading-edge shock wave and the compression waves generated from the body surface. Sullivan[1] obtained similar solutions for the inviscid hypersonic flow on cusped concave surfaces and showed that they are the correct first approximation over a region to the exact inviscid equations in the limit of infinite freestream Mach number. A detailed comparison of the similar solutions with other approximate inviscid theories was given later.[2] It is often considered that the leading-edge bluntness or the boundary-layer displacement effect on concave surface flows is much less important. On physical grounds, this is reasonable to expect since the body incidence controls the flow everywhere on such surfaces except in the vicinity of the leading edge. Rigorous theoretical investigation of such flows, instead of assuming the leading-edge effect to be unimportant has received attention only recently. For the case of boundary-layer displacement effect, Stollery[3] showed that Cheng's zeroth-order strong interaction theory[4] leads to quantitatively unrealistic oscillatory results when applied to concave surfaces. An alternative approach using the tangent wedge rule in place of the Newton-Busemann pressure law used in Cheng's theory was suggested. The modified analysis using the tangent wedge rule suppressed the oscillatory behavior and a smooth approach to downstream conditions was obtained. Later, the method was extended[5] to the case of a blunt flat plate at incidence for which Cheng's zeroth-order theory is known to yield oscillatory results for both pressure and shock shapes.

In this Note, both Cheng's theory and its modified version using tangent wedge rule are studied for power-law concave surface flows with leading-edge bluntness. It is demonstrated that Cheng's theory yields highly oscillatory results for concave surfaces with blunt leading edge. As in the case of viscous interaction,[3] the tangent wedge analysis is found to predict a smooth transition from the leading-edge blast wave effect to the downstream asymptotic conditions. The alternative use of the tangent wedge formula cannot be justified strictly from theoretical considerations, since it neglects the centrifugal pressure rise on the surface. The implications of this are discussed in detail.[9] Though at present no experimental support is available for the analysis, the good agreement[3,9] with the experimental results obtained for concave surfaces with sharp leading-edge using the tangent wedge formula suggests that the present analysis may be useful in making first estimates, since the effects of the nose bluntness and the boundary-layer displacement are similar.

Analysis

Newton-Busemann Analysis

In the limit of freestream Mach number (M_∞) tending to infinity and the ratio of specific heats (γ) tending to unity, Cheng's pressure area relationship for the hypersonic flow past a blunt nosed slender body is given by

$$p_e(y_e - y_b) = [(\gamma-1)D_n]/2 \tag{1}$$

where p_e is the pressure (assumed constant across the entropy layer), y_e the edge of the entropy layer, y_b the geometric body shape, and D_N the drag of the blunt leading edge. Equation (1), along with a suitable pressure law, determines the problem completely for a given afterbody shape. For the Newton-Busemann rule used in cheng's theory, the pressure is given by

$$P = \frac{p_e}{p_\infty} = \gamma M_\infty^2 \frac{\mathrm{d}}{\mathrm{d}x}\left[y_e \frac{\mathrm{d}y_e}{\mathrm{d}x}\right] \tag{2}$$

where p_∞ is the freestream pressure. Substituting for p_e in Eq. (1) and using a nose drag coefficient $C_{DN}(=2D_N/\rho_\infty U_\infty^2 t)$ based on the leading-edge thickness t, for the particular case of a power law afterbody shape ($y_b \alpha x^n$) we get

$$(z-\zeta^n)\ (\mathrm{d}/\mathrm{d}\zeta)\left[z\frac{\mathrm{d}z}{\mathrm{d}\zeta}\right] = 1 \tag{3}$$

where

$$z = y_e/\theta\ell,\ \zeta = x/\ell,\ \theta = \text{constant}$$

$$\ell = (\gamma-1)C_{DN}t/4\theta^3,\ \text{length scale}$$

For a blunt plate at incidence ($n=1$), the results and the asymptotic behavior of Eq. (3) for $\zeta \to \infty$ have been given by Cheng. Here, concave surfaces ($n>1$) with leading-edge bluntness are considered. Equation (3) must be integrated numerically starting near the leading edge using the series expansion and integrating downstream. For $\zeta \to 0$, it may be shown by expanding in series, the solution valid near the leading edge is

$$z = (9/2)^{1/3}\zeta^{2/3} + \frac{2}{9n^2+3n}\zeta^n + \ldots \tag{4}$$

Similarly for large ζ, it can be shown that z behaves as

$$z \approx \zeta^n + \frac{1}{n(2n-1)}\zeta^{2-2n} + A\zeta^{(4-7n/4)}\cos\left[\frac{2n(2n-1)}{3n-2}\zeta^{(3n-2/2)} + B\right] + \ldots \tag{5}$$

where A and B are arbitrary constants. In view of the third term, it follows that the shock approaches the body surface in an oscillatory manner. The corresponding behavior for the pressure is given by

$$\frac{P}{\gamma M_\infty^2\theta^2} = (z-\zeta^n)^{-1} = n(2n-1)\zeta^{2n-2}\left[1 - An(2n-1)\zeta^{(n-4)/4}\cos\left[\frac{2n(2n-1)}{3n-2}\zeta^{(3n-2/2)} + B\right] + \ldots\right] \tag{6}$$

For the particular case of a blunted wedge ($n=1$), Eqs. (5) and (6) reduce to the familiar results obtained in Ref. 4 for shock shape and pressure.

Modified Tangent Wedge Analysis

In this analysis, Cheng's pressure area relation given by Eq. (1) is used along with the tangent wedge rule to determine the pressure on the surface. The local pressure at any point on the effective body surface defined by the edge of the entropy layer is given by

$$P = \frac{p_e}{p_\infty} = 1 + \gamma M_\infty^2\left[\frac{\mathrm{d}y_e}{\mathrm{d}x}\right]^2\left[\frac{\gamma+1}{4} + \left[\left[\frac{\gamma+1}{4}\right]^2 + \frac{1}{M_\infty^2(\mathrm{d}y_e/\mathrm{d}x)^2}\right]^{1/2}\right] \tag{7}$$

After simplification, Eq. (7) can be written as

$$\frac{\mathrm{d}z}{\mathrm{d}\zeta} = \frac{P-1}{\gamma M_\infty^2\theta^2}\left[\frac{\gamma-1}{\gamma M_\infty^2\theta^2} + \frac{(\gamma+1)P}{2\gamma M_\infty^2\theta^2}\right]^{-1/2} \tag{8}$$

where $z = y_e\theta/\ell$. For surfaces described by $z_w = \zeta^n$, Eq. (1) written in terms of variables z, ζ, and P becomes

$$(z-\zeta^n)\frac{P}{\gamma M_\infty^2\theta^2} = 1 \tag{9}$$

Equations (8) and (9) can be solved for given body shape and the unknowns shock shape z and pressure P can be determined. For the limiting case of $M_\infty\theta\to\infty$, they can be combined to give

$$(z-\zeta^n)\left(\frac{dz}{d\zeta}\right)^2=\frac{2}{\gamma+1} \tag{10}$$

For the case of a blunt flat plate at incidence, the equations can be integrated analytically to give closed form solution.[6] For other shapes, the equations are to be integrated numerically starting near the leading edge using the series expansion and marching downstream. The series expansion valid near the leading edge is obtained by expanding Eq. (7) for $\zeta\to 0$ and the result is

$$z\approx\left[\frac{9}{2(\gamma+1)}\right]^{1/3}\zeta^{2/3}+\frac{1}{1+3n}\zeta^n+\ldots \tag{11}$$

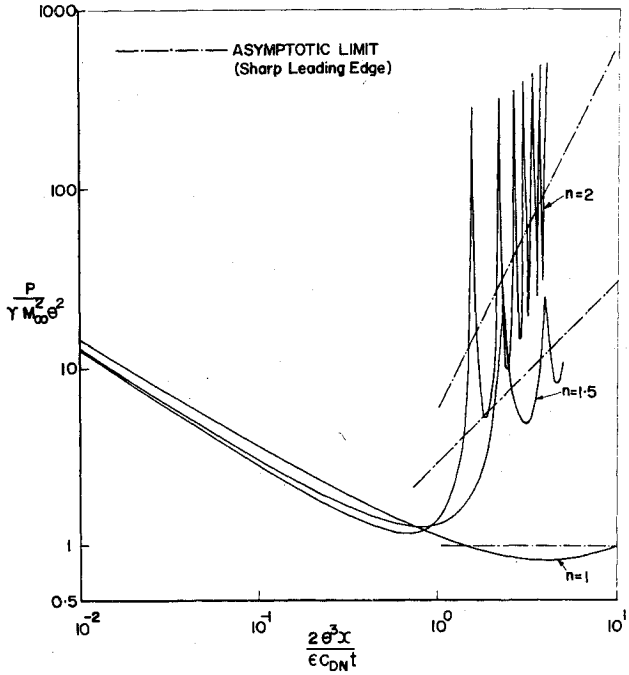

Fig. 1 Results of Cheng's theory for concave surfaces ($z_w=\zeta^n$) with blunt leading edge.

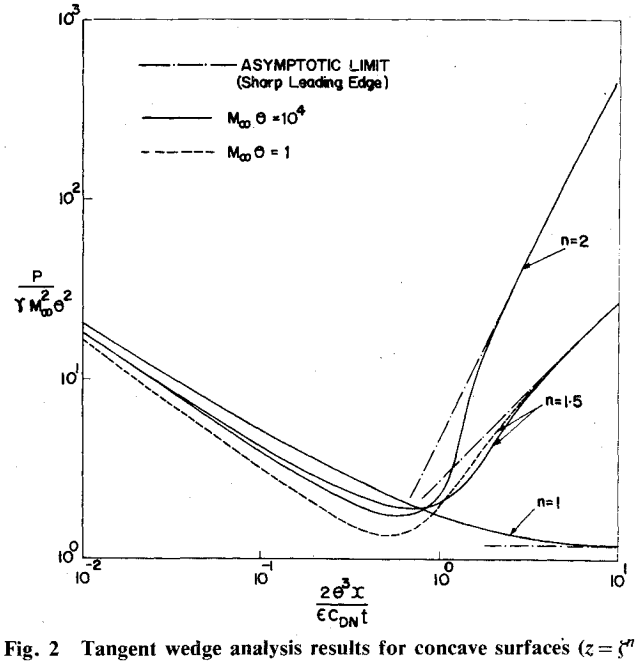

Fig. 2 Tangent wedge analysis results for concave surfaces ($z=\zeta^n$) with blunt leading edge ($\gamma=1.4$).

Numerical Results and Discussion

The governing equations for both Cheng's and the modified tangent wedge analysis were integrated by Runge-Kutta method on an ICL 1905 computer using double precision arithmetic. The integration was started at a point close to the leading edge making use of the series expansion for $\zeta\to 0$. The results of the integration for the surface pressure are shown in Figs. 1 and 2. From Fig. 1, it may be observed that the mild oscillatory behavior predicted by Cheng's theory for a blunt flat plate at incidence[4] appears to become severe for concave surfaces. This behavior is similar to that found for the case for viscous interaction by Stollery[3,5] but the amplitude of oscillations appears to be much higher. For the surface $z_w=\zeta^2$, oscillations are poorly damped even after about 7 cycles. Near the leading edge where the distribution is similar to that on a flat plate, the pressure is decreasing as the entropy layer produced by the blunt leading edge is thickening. At a point downstream, the pressure reaches a minimum and then starts increasing under the influence of the body incidence. Correspondingly, the entropy layer thins down to a minimum and starts increasing again. Following this, the entropy layer undergoes successive thinning and thickening until eventually, the oscillations are damped far downstream.

The results of the tangent wedge analysis are presented in Fig. 2. The results are completely nonoscillatory and the downstream asymptotic conditions are reached monotonically. As n increases, the surface incidence dominates and the sharp leading edge results are approached much earlier. The effect of the incidence parameter $M_\infty\theta$ is shown for the surface $z_w=\zeta^{1.5}$. For $M_\infty\theta=1$, it is observed that the minimum value of the nondimensional pressure is lower than that for $M_\infty\theta=10^4$. The results of the tangent wedge analysis suggest that the effect of the blunt leading edge is to cause a lag in the pressure rise compared to that for a sharp leading edge. This lag effect is similar to that observed experimentally by Richey[7] for the case of displacement interaction on concave surfaces. In general, the effect of the leading-edge bluntness and the boundary-layer displacement can be considered to be similar since both contain gas particles at high temperature and low density. The entropy layer of the blunt leading edge initially grows, reaches a maximum thickness where the pressure is a minimum, and then starts thinning downstream gradually under the influence of the body incidence and increasing pressure. This behavior is similar to the supercritical behavior of the boundary-layer on a concave surface discussed by Mohammadian[8] and Murthy.[9]

The physical reality of such poorly damped oscillations predicted by Cheng's zeroth-order theory is highly doubtful. Far downstream, other effects such as afterbody drag, etc., normally considered to be of higher order, will strongly damp the oscillations.[9] The modified analysis using the tangent wedge rule which predicts a nonoscillatory approach can be used to obtain first estimates on concave surfaces with leading-edge bluntness. Good agreement of the tangent wedge analysis with pressure measurements has been observed[8,9] for the case of concave surface with boundary-layer displacement effect.

The oscillatory behavior in shock shape and pressure suggested by Eqs. (5) and (6) has also been demonstrated in Refs. 10 and 11 by considering the equivalent problem of an intense explosion with moving contact surface. It was also shown by extending the analysis to a higher degree that for a blunted wedge, the higher order theory almost eliminates the oscillatory behavior predicted by the zeroth-order theory. This suggests that such an improvement over the zeroth-order

theory should also be possible for concave surface flows with leading-edge bluntness.

References

[1] Sullivan, P. A., "Inviscid Hypersonic Flow on Cusped Concave Surfaces," *Journal of Fluid Mechanics*, Vol. 24,pt. 1, 1966, pp. 99-112.

[2] Sullivan, P. A., "A Discussion of Approximate Theories for Inviscid Hypersonic Flow on Concave Surfaces," Rept. 140, 1970, Institute for Aerospace Studies, University of Toronto, Toronto, Canada.

[3] Stollery, J. L., "Hypersonic Viscous Interaction on Curved Surfaces," *Journal of Fluid Mechanics*, Vol. 43, 1970, pt. 3, pp. 497-511.

[4] Cheng, H. K., Hall, J. G., Golian, T. C. and Hertzberg, A., "Boundary-Layer Displacement and Leading Edge Bluntness Effects in High Temperature Hypersonic Flows," *Journal of the Aerospace Sciences*, Vol. 28, May 1961, pp. 353-381.

[5] Stollery, J. L., Pimputkar, S. and Bates, L.,[11] "Hypersonic Viscous Interaction," *Fluid Dynamics Transactions*, Polish Academy of Sciences, Vol. 6, 1971, pp. 545-562.

[6] Murthy, A. V., "Hypersonic Flow over Blunted Slender Wedges," *Journal of Aircraft*, Vol. 11, April 1974, pp. 249-251.

[7] Richey, G. K., "An Analysis of the Laminar Boundary-Layer Inviscid Flow Interaction at Hypersonic Speeds," AIAA Paper 65-569, Colorado Springs, Colo., 1965.

[8] Mohammadian, S., "Viscous Interaction over Concave and Convex Surfaces at Hypersonic Speeds," *Journal of Fluid Mechanics*, Vol. 55, 1972, pt. 1, pp. 163-175.

[9] Murthy, A. V., "Studies in Hypersonic Viscous Interactions," Ph.D. thesis, Dec. 1972, Dept. of Aerodynamics, Cranfield Institute of Technology, Bedford, England.

[10] Cheng, H. K. and Kirsch, J. W., "On the Gas Dynamics of an Intense Explosion with an Expanding Contact Surface," *Journal of Fluid Mechanics*, Vol. 39, pt. 2, 1969, pp. 289-305.

[11] Cheng, H. K., Kirsch, J. W., and Lee, R. S., "On the Reattachement of a Shock Layer Produced by an Instantaneous Energy Release," *Journal of Fluid Mechanics*, Vol. 48, pt. 2 1971, pp. 241-263.

Solution of Lateral Vibration of a Cantilever by Parameter Differentiation

J. P. Chiou*
University of Detroit, Detroit, Mich.

and

T. Y. Na†
University of Michigan—Dearborn, Dearborn, Mich.

A NONITERATIVE method for the solution of nonlinear algebraic equations has recently been developed by Kane[1] and Yakolev.[2] Briefly, the solution of a nonlinear algebraic equation

$$F(x)=0 \tag{1}$$

can be obtained as follows: First, an arbitrary first approximation of the solution of Eq. (1), say x_1, is chosen. A new equation is then defined as

$$F(x)=F(x_1)\ (1-\tau) \tag{2}$$

where τ is a parameter which changes from 0 to 1. When τ equals to zero, the solution of Eq. (2) becomes x_1, the first approximation of the solution of Eq. (1). When τ equals 1, Eq. (2) is reduced to Eq. (1), which means the solution of Eq. (2) becomes the solution of Eq. (1). For this reason, the solution of Eq. (2), as τ changes from 0 to 1, is expected to change from x_1 to the solution of Eq. (1). This points out the need of a differential equation of $dx/d\tau$, originating from Eq. (2). Such an equation can be obtained by differentiating Eq. (2) with respect to τ. We therefore get

$$F'(x)\,dx/d\tau=-F(x_1) \tag{3}$$

subject to the initial condition

$$\tau=0\text{:}\ x=x_1$$

By integrating Eq. (3) from 0 to 1, the solution of Eq. (3) will be changed from x_1 (at $\tau=0$) to the solution of Eq. (1) (at $\tau=1$). The merit of the method is that it eliminates the iteration process. It should be noted that Eq. (3) is a variation of the interative Newton-Raphson method,

$$x_{k+1}=x_k-F(x_k)/F'(x_k)$$

As a result of multiplicity of solutions for nonlinear algebraic equations, the specific solution approached will depend on the value of x_1 selected. While this property might pose difficulties for certain problems in the selection of x_1 where only *one* of the solutions is physically meaningful, it can be used to the advantage of the engineer for other problems where this method can be used to systematically search for all possible solutions. An example will be given in this Note to illustrate this particular feature of the method.

Consider a uniform Bernoulli-Euler beam of length L clamped at one end and subjected at the other end to a constant tensile follower force P, as shown in Fig. 1. The amplitude of s small transverse vibration about the x-axis is governed by the differential equation[3]

$$EI\frac{\partial^4 y}{\partial x^4}-P\frac{\partial^2 y}{\partial x^2}+\rho\frac{\partial^2 y}{\partial t^2}=0 \tag{4}$$

where E, I, and ρ are, respectively, the Young's modulus, the moment of inertia, and the density. By introducing the dimensionless variables

$$\xi=\frac{x}{\ell}\,,\quad \tau=t\left(\frac{EI}{\rho\ell^4}\right)^{1/2},\quad k^2=\frac{P\ell^2}{EI} \tag{5}$$

Eq. (4) becomes

$$(\partial^4 y/\partial\xi^4)-k^2(\partial^2 y/\partial\xi^2)+\partial^2 y/\partial\tau^2=0 \tag{6}$$

Following Anderson and King,[3] the solution is written in the form:

$$y(\xi,\tau)=Y(\xi)\sin\omega\tau \tag{7}$$

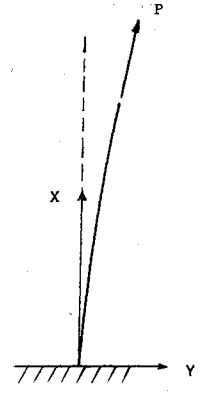

Fig. 1 The cantilever.

Received December 5, 1974; revision received March 21, 1975.
Index categories: Aircraft Structural Design (including Loads).

*Associate Professor of Mechanical Engineering.
†Professor of Mechanical Engineering. Member AIAA.